HHS Public Access

Author manuscript

Anal Chem. Author manuscript; available in PMC 2023 June 21.

Published in final edited form as:

Anal Chem. 2023 January 31; 95(4): 2532–2539. doi:10.1021/acs.analchem.2c04986.

Exploring an Alternative Cysteine-Reactive Chemistry to Enable Proteome-Wide PPI Analysis by Cross-Linking Mass Spectrometry

Fenglong Jiao[1], **Leah J. Salituro**[2], **Clinton Yu**[1], **Craig B. Gutierrez**[1], **Scott D. Rychnovsky**[2], **Lan Huang**[1,*]

[1]Department of Physiology and Biophysics, University of California, Irvine, CA 92697

[2]Department of Chemistry, University of California, Irvine, CA 92697

Abstract

The development of MS-cleavable cross-linking mass spectrometry (XL-MS) has enabled effective capture and identification of endogenous protein-protein interactions (PPIs) and their residue contacts at the global scale without cell engineering. So far, only lysine-reactive cross-linkers have been successfully applied for proteome-wide PPI profiling. However, lysine cross-linkers alone cannot uncover the complete PPI map in cells. Previously we have developed a maleimide-based cysteine-reactive MS-cleavable cross-linker (bismaleimide sulfoxide(BMSO)) that is effective for mapping PPIs of protein complexes to yield interaction contacts complementary to lysine-reactive reagents. While successful, the hydrolysis and limited selectivity of maleimides at physiological pH make their applications in proteome-wide XL-MS challenging. To enable global PPI mapping, we have explored an alternative cysteine labeling chemistry, and thus designed and synthesized a sulfoxide-containing MS-cleavable haloacetamide-based cross-linker, Dibromoacetamide sulfOxide (DBrASO). Our results have demonstrated that DBrASO cross-linked peptides display the same fragmentation characteristics as other sulfoxide-containing MS-cleavable cross-linkers, permitting their unambiguous identification by MS^n. In combination with a newly developed two-dimensional peptide fractionation method, we have successfully performed DBrASO-based XL-MS analysis of HEK293 cell lysates and demonstrated its capability to complement lysine-reactive reagents and expand PPI coverage at the systems-level.

Graphical Abstract

*Correspondence should be addressed to Dr. Lan Huang (lanhuang@uci.edu), Medical Science I, D233, Department of Physiology & Biophysics, University of California, Irvine, Irvine, CA 92697-4560, Phone: (949) 824-8548, Fax: (949) 824-8540.

Conflict of Interest

The authors declare no conflict of interest

Supporting Information for Publication

- Additional experimental details including materials and methods;
- Supplemental figures and legends describing synthesis of DBrASO and analyses of DBrASO cross-linked synthetic peptide, standard protein and cell lysates;
- Supplemental tables detailing the identification of cross-linked peptides, C-C linkages, distance mapping of cross-links, and CORUM protein complex analysis.

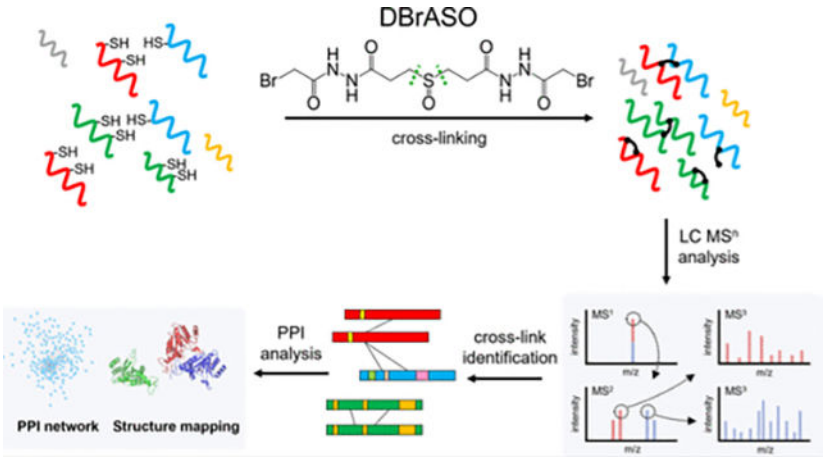

Introduction

Protein-protein interactions (PPIs) are essential for the assembly of protein complexes, the active molecular modules for controlling cellular functionality and modulating physiological states.[1,2] In recent years, cross-linking mass spectrometry (XL-MS) has been proven effective for studying PPIs and elucidating architectures of protein complexes *in vitro* and *in vivo* at the systems-level.[2–6] Compared to other PPI methods, XL-MS enables the capture of endogenous PPIs without cell engineering. Identification of cross-linked peptides concurrently reveals PPI identities and interaction contacts at specific residues, which provide distance constraints defined by a given cross-linker to help refine existing structures and elucidate structures of protein complexes through computational modeling.[5,7,8] In particular, the development of MS-cleavable cross-linkers have significantly advanced global PPI mapping to define the modularity and dynamics of cellular networks.[5,9–15] This is due to the capability of MS-cleavable cross-linkers to provide simplified MS data for effective database searching, permitting cross-link identification with speed and accuracy. While successful, current proteome-wide XL-MS studies have all been relying on lysine-reactive cross-linkers. Although multiple cross-linking chemistries have been explored for XL-MS studies,[5,8,16,17] lysine-reactive reagents remain the most popular. However, lysine-based XL-MS studies have only uncovered a fraction of proteomes.[10,11,13–15] It is evident that additional cross-linking chemistries are important to expand PPI coverages and complement existing reagents.[5,18,19]

In addition to lysine and acidic residues, cysteine is an attractive and unique amino acid owing to its critical importance in protein structure and function. Since the sulfhydryl group is highly reactive and can form disulfide bonds, cysteines modulate protein structures in multiple ways including protein dimerization, metal coordination, redox regulation, and thermal stability.[20–23] Cysteines can be labeled by many electrophilic reagents with high specificity and efficiency, which has been widely used in proteomic studies. While cysteine is one of the least abundant amino acids, it is often found at functional sites of proteins and its evolution appears to be highly regulated in proteins.[21] Thus, cysteine cross-linking is expected to provide additional molecular details to help advance our understanding of protein interactions and structures. To enable cysteine-based XL-MS analysis, we have

previously developed the homobifunctional MS-cleavable cysteine-reactive cross-linker bismaleimide sulfoxide (BMSO), which has been successfully applied to define protein interactions and complement both lysine and acidic residue reactive reagents to expand PPI coverages.[8,19] In addition, the multichemistry-based XL-MS approach was shown to facilitate the elucidation of the architectures of protein complexes by improving structural modeling with significantly increased precision.[8] While maleimide chemistry has the fastest kinetics among the commonly used cysteine-reactive groups,[24] maleimide-labeled products can undergo retro-Michael addition and thiol exchange under physiological conditions.[25] In addition, maleimides are prone to hydrolysis, which leads to the formation of ring-opened maleamic acids that are inactive to thiols.[19] Finally, maleimide chemistry can be promiscuous, capable of labeling lysines at alkaline pH[26] and resulting in unexpected complexity. Therefore, the exploration of alternative cysteine labeling chemistries with higher specificity and less complexity would be advantageous to enable robust profiling of cysteine XL-proteomes to expand PPI mapping.

Apart from maleimide, haloacetamide chemistry is commonly employed for cysteine labeling/alkylation for protein identification and activity profiling in proteomics studies.[27,28] Although haloacetamides have slower cysteine reactivity, they are advantageous as they do not hydrolyze, are more residue specific, and produce more homogenous cross-linked products for improved identification and quantitation. Thus, we have developed dibromoacetamide sulfoxide (DBrASO (, aka, 3,3’-sulfinylbis(N’-(2-bromoacetyl)propanehydrazide), by coupling bromoacetamide functional groups with sulfoxide-based MS-cleavability for unambiguous cross-link identification.[5,18,19,29] Here, we demonstrate that DBrASO is an effective cysteine-reactive cross-linker for both simple and complex samples. Importantly, we have established an integrated DBrASO-based XL-MS analytical workflow coupled with a newly developed two-dimensional fractionation method and LC-MS^n data acquisition for complex PPI profiling.[15] This platform has been successfully applied to cross-link HEK293 cell lysates, yielding a total of 11,478 unique cross-linked peptides describing an XL-proteome containing 2297 proteins. To the best of our knowledge, this work describes the first proteome-wide XL-MS study using a cysteine cross-linker. Our results have demonstrated that DBrASO is effective for global XL-MS analysis and represents an attractive reagent to complement existing lysine-reactive cross-linkers for comprehensive PPI mapping at the systems-level.

EXPERIMENTAL PROCEDURES

Materials and Reagents

General chemicals were purchased from Fisher Scientific or VWR International. Bovine serum albumin (≥96% purity) was purchased from Sigma-Aldrich. Sequencing grade trypsin was purchased from Promega (Madison, WI). Ac-LR9 peptide (Ac-LADVCAHER, 98% purity) was custom ordered from Biomatik (Wilmington, DE).

Synthesis and Characterization of DBrASO

DBrASO was designed and synthesized based on our previously developed acidic-residue cross-linker, dihydrazide sulfoxide (DHSO)[18] (Figure S1). The details are described in the Supporting Methods.

DBrASO Cross-linking of Synthetic Peptide and Proteins

DBrASO cross-linking of synthetic peptide Ac-LR9, BSA and 293 cell lysates was carried out similarly as described[15,19] (Supporting Methods).

Cross-link Identification and Data Analysis

DBrASO cross-linked proteins were digested by LyC-trypsin as previously described.[15] Cross-linked peptides of BSA were directly subjected to LC MS^n analysis, while cross-linked peptides from HECK 293 cell lysates were first fractionated by a SEC-HpHt method.[15] LC-MS^n analysis was carried out using an UltiMate 3000 RSLC coupled with an Orbitrap Fusion Lumos mass spectrometer for the identification of DBrASO cross-linked peptides. Three biological replicates were performed for each type of XL-MS experiments. PPI analysis and structural mapping were performed similarly as previously described[14,15] (Supporting Methods).

RESULTS AND DISCUSSION

Design and Synthesis of a Novel MS-Cleavable Homobifunctional Cysteine Cross-Linker

To improve the specificity and homogeneity of cysteine cross-linking, we sought to incorporate an alternative sulfhydryl chemistry, i.e., haloacetamide group to create a novel sulfoxide-containing MS-cleavable cysteine-reactive homobifunctional cross-linker, similar to BMSO (Figure 1A). Haloacetamides such as iodoacetamide and chloroacetamide have been commonly used for cysteine alkylation prior to enzymatic digestion in proteomics studies.[27,30] In this work, we selected bromoacetamide as the reactive group due to its comparable reactivity to iodoacetamide and ease of handling during synthesis.[31] Thus, we designed DBrASO, a homobifunctional cysteine cross-linker composed of two bromoacetamide groups connected by a spacer arm containing a central sulfoxide group adjacent symmetrical MS-cleavable C-S bonds (Figure 1B). The design of DBrASO was built upon the DHSO cross-linker, and the synthesis incorporated a late-stage sulfide to sulfoxide oxidation to minimize undesired reactivity (Supporting Methods and Figure S1). DBrASO has a spacer arm length of 16.4 Å, which is considerably shorter than BMSO (24.2 Å) and well within the distance range suited for mapping PPIs.[5]

MS Characterization of DBrASO Cross-linked Peptides

While DBrASO cross-linking is expected to result in different types of cross-linked peptides, we focused on the characterization of DBrASO inter-linked peptides due to their importance in delineating protein interactions and structures[5]. Similar to other residue-specific sulfoxide-containing cross-linkers such as DSSO and BMSO,[8,19,29,32,33] cleavage of either MS-cleavable C-S bond physically separates the two cross-linked peptide constituents, yielding peptide fragment ion pairs (i.e., α_A/β_S or α_S/β_A). These resulting peptide fragments

are modified with alkene (A) or sulfenic acid (S) moieties, remnants of DBrASO following collision-induced dissociation (CID). The sulfenic moiety typically undergoes dehydration to become a more stable and dominant unsaturated thiol (T) moiety.[19] Therefore, the two dominant fragment pairs for a DBrASO cross-linked peptide α-β are expected to be α_A/β_T and α_T/β_A (Figure 1C), which are then subjected to MS^3 analysis for unambiguous identification of cross-linked peptides.

The fragmentation characteristics of DBrASO cross-linked peptides were first evaluated using a cysteine-containing synthetic peptide Ac-LR9 (i.e., Ac-LADVCAHER). MS^2 analysis of the DBrASO cross-linked Ac-LR9 homodimer (m/z 603.7698^{4+}) resulted in three dominant fragments: α_A (m/z 591.2379^{2+}), α_T (m/z 607.2593^{2+}), and α_S (m/z 616.2654^{2+}), with the alkene- and thiol-modified peptides being most dominant as anticipated (Figure S2). Subsequent MS^3 analyses of α_A and α_T determined the C-C cross-link in the Ac-LR9 homodimer. These results demonstrate that CID-induced fragmentation of the DBrASO cross-linked peptide is similar to other sulfoxide-containing MS-cleavable cross-linked peptides.[5]

DBrASO XL-MS Analysis of BSA

To assess the efficiency of DBrASO for protein cross-linking, we cross-linked standard protein bovine serum albumin (BSA) due to its high cysteine content and common use in XL-MS studies.[18,19] To characterize DBrASO cross-linking of BSA, LC-MS^n analysis was employed to identify DBrASO cross-linked peptides. As an example, MS^n analysis of a representative DBrASO inter-linked peptide α-β of BSA (m/z 676.5522^{4+}) is illustrated in Figure 2. Fragmentation of the cross-link during MS^2 produced two major ion pairs, i.e., α_A/β_T and α_T/β_A, further confirming the expected fragmentation characteristics of DBrASO cross-linked peptides. MS^3 sequencing of α_A (m/z 571.2717^{2+}) and β_T (m/z 772.8250^{2+}) determined their peptide sequences as $^{286}SHC_AIAEVEK^{294}$ and $^{311}YIC_TDNQDTISSK^{322}$ respectively. Together, integration of MS^1, MS^2, and MS^3 spectral data unambiguously identified a cross-link between C288-C313 of BSA. In total, 69 unique C-C linkages were identified from three biological replicates (Table S1). 59.4% of the unique C-C linkages were found in all three replicates, displaying similar reproducibility to other sulfoxide-containing cross-linkers.[8,19] To evaluate the interaction coverage observed by DBrASO, identified C-C linkages were plotted on a published BSA crystal structure (PDB: 4F5S) (Figure 3A). In total, 27 out of 35 cysteines were found to be cross-linked, indicating a high cysteine coverage. Based on the length of the DBrASO space arm (16.4 Å) and cysteine side chains (2.8 Å), as well as considering protein flexibility and dynamics, the maximum Cα-Cα distance between two DBrASO cross-linkable cysteine residues would be estimated to be ≤ 40 Å. Out of the 69 C-C linkages, 91.3% of them were considered satisfactory as they are below the max distance threshold (Figure 3B), supporting the validity of the identified cross-links.

To examine whether the differences in cysteine labeling efficiency between haloacetamide and maleimide functional groups could impact BSA cross-linking, we performed BMSO cross-linking on BSA using the same conditions as DBrASO. A total of 75 BMSO C-C linkages were identified from 3 biological replicates, and 92% of them were considered

satisfactory (≤ 45 Å) (Figure 3B). Although the total number of unique C-C linkages identified for each linker was similar, they only shared 23.1% of identified linkages in common (Figure S3)–significantly lower than the overlap among their respective biological replicates. The limited commonality suggests discernable differences between the efficiency of DBrASO and BMSO cross-linking. Although DBrASO (16.4 Å) is shorter than BMSO (24.2 Å), the average distances of their cross-links were 23.9 ± 13.3 Å (24.6 Å median) for DBrASO and 26.9 ± 13.6 Å (28.6 Å median) for BMSO. Out of the 42 C-C linkages that were uniquely identified by DBrASO, five were longer than 40 Å. For comparison, 12 out of the 48 BMSO unique cross-linked linkages were longer than 40 Å and six of them were longer than 45 Å. Therefore, we suspect that the observed differences between DBrASO and BMSO cross-links of BSA are more likely due to the differences in the two linkers including their physiochemical properties, reaction kinetics, tendency to hydrolyze, product heterogeneity and accessibility to cross-linkable sites. In addition, owing to the structural differences in BMSO and DBrASO cross-links, there will be variability in the separation and detectability of DBrASO and BMSO cross-linked peptides during LC MS^n analysis. Taken together, our results demonstrate that DBrASO is effective for protein cross-linking and yields cross-links complementary to BMSO, thus increasing PPI coverages through C-C linkages.

DBrASO XL-MS Analysis of HEK293 Cell Lysates

Recent advances in XL-MS technologies have successfully enabled proteome-wide XL-MS studies using lysine-reactive cross-linkers.[10,11,14,15,34,35] However, whether and how other cross-linking chemistries complement lysine-reactive reagents in proteome-wide PPI mapping have not yet been investigated. Previous XL-MS analyses of proteins and protein complexes have proven the benefits of using multiple cross-linking chemistries to expand PPI mapping and enhance the precision of structural modeling.[8,18,19,36,37] To explore the feasibility of cysteine-reactive cross-linkers for proteome-wide XL-MS studies, we performed DBrASO cross-linking of HEK293 cell lysates (Figure S4). To enhance the detectability and identification of cross-linked peptides from complex samples, we employed a recently developed two-dimensional fractionation method by coupling peptide size exclusion chromatography (SEC) with tip-based high-pH reverse phase (HpHt) separation (SEC-HpHt)[15] to enrich DBrASO cross-linked peptides from cell lysate digests. This workflow resulted in a total of 12 SEC-HpHt fractions for each proteome-wide XL-MS experiment. Here, we performed three biological replicates, yielding a total of 36 fractions for LC-MS^n analysis. As a result, 27,809 cross-link peptide spectrum match (CSMs) were obtained, corresponding to 11,478 unique DBrASO cross-linked peptides that represent 8222 unique C-C linkages from 2297 human proteins (Table S2). Here, the 8222 unique C-C linkages describe 1037 interprotein and 7185 intraprotein interactions.

Comparisons of DBrASO and DSSO XL-Proteomes

To illustrate the differences between cysteine and lysine cross-linking chemistries, we compared the identified 2297 DBrASO XL-MS proteome with our previously published DSSO XL-proteome of HEK293 cell lysates.[15] Similar to DSSO, DBrASO cross-linked proteins were enriched in various subcellular compartments, including nucleus, cytosol and mitochondria (Figure 4A). Of the proteins identified by DBrASO cross-linking, 997

were shared with the DSSO XL-proteome. The remaining 1300 proteins were unique to DBrASO, expanding the overall proteome coverage (Figure 4B). Gene Ontology (GO) analysis indicated that similar cellular components were found for both DBrASO and DSSO XL-proteomes, with an enrichment in mitochondrial matrix, focal adhesion, cell-substrate junction, and ribosomes. In addition, similar biological processes, such as RNA metabolic process and ribonucleoprotein complex biogenesis, and molecular functions, such as protein binding or kinase activity, were enriched in both XL-MS datasets (Figure S5).

We next plotted the abundance distribution of XL-proteomes using the intensity-based absolute quantification (iBAQ) values of the HEK293 MS proteome in ProteomicsDB.[38] Out of the 2297 DBrASO-dentified proteins, 2152 were correlated with iBAQ values, and their distribution indicated that high-abundance proteins were well-represented in the cysteine XL-proteome (Figure 4C), similar to lysine XL-proteomes.[14,15] This is somewhat expected, as the yield of cross-linking data is substoichiometric and heavily dependent on protein abundance. Interestingly, DBrASO appeared to uncover slightly more low-abundance proteins (Log_{10}iBAQ≤5) than DSSO[15] (556 vs. 275), suggesting that cysteine-reactive cross-linkers may be helpful in capturing certain lower abundance PPIs. To understand the relationship between cysteine occurrence and protein abundance, we plotted their distribution correlation (Figure S6). As shown, the average occurrence of cysteines did not correlate to protein abundance. Next, we compared the total number of interprotein and intraprotein cross-links containing low-abundance proteins (Log_{10}iBAQ≤5). Among the 891 unique C-C linkages involving the 556 DBrASO cross-linked low abundance proteins, 84 represent interprotein and 807 represent intraprotein cross-links. In comparison, among the 591 unique K-K linkages from the 275 DSSO cross-linked proteins, 286 depict interprotein and 305 represent intraprotein cross-links. This indicates that most of the cross-links containing low abundance proteins from DBrASO XL-data were obtained through intraprotein interactions. As the occurrence of lysines is significantly higher than that of cysteines in the proteome and on protein interaction interfaces, higher number of interprotein cross-links would be identified with DSSO than DBrASO. For the same reason, the total number of DSSO cross-links from high abundance proteins would be much higher than that of DBrASO, leading to less identification of DSSO cross-links from low abundance proteins. Therefore, the observed differences in DBrASO and DSSO XL-proteomes are likely attributed to multiple factors including cross-linking chemistry, the availability of cross-linkable residues, and the detectability of resulting cross-linked peptides. Nonetheless, our results suggest DBrASO can capture additional PPIs to help expand proteome coverage in XL-MS experiments.

Examination of Cross-links by Structural Mapping

The DBrASO XL-proteome of HEK293 cell lysates is composed of 2297 proteins, in which 975 CORUM protein complexes were found and 74.5% of them were identified with more than 50% protein composition of each protein complex (Table S3A). Based on the number of C-C linkages, the most representative complexes are the cytoplasmic ribosome, CCT, 26S proteasome, and pre-mRNA spliceosome complexes. To assess the validity of DBrASO cross-links, a total of 1380 C-C linkages (879 intraprotein and 501 interprotein) were mapped onto available high-resolution structures of 126 protein complexes (Table

S3B). While 717 out of the 879 intra-protein C-C linkages (81.6%) corresponded to Cα-Cα distances below the DBrASO threshold (≤ 40 Å), the majority of the 501 interprotein C-C linkages were found to be nonsatisfactory. However, it is noted that 97% of the violating inter-protein cross-links were determined to be associated with ribosomal proteins (460/475, Table S3B). This is not surprising as the ribosomal complex is known to be highly dynamic,[39] and various lysine-based XL-MS datasets of purified samples and cell lysates have revealed a large number of non-satisfactory inter-protein cross-links from ribosomal proteins.[13,15] Therefore, DBrASO XL data further supports the structural plasticity of the ribosomal complex.

A well-represented complex in our dataset is the eight-subunit CCT complex, identified with 153 C-C cross-links describing 148 intra-subunit and 5 intersubunit interactions involving all 8 subunits. Out of the 145 C-C linkages that were able to be mapped onto the CCT complex structure (PDB: 7LUP), the majority (74%) were satisfied with the Cα-Cα distances ≤ 40 Å (Figure 5A,D). For the 26S proteasome (PDB:5GJR) and pre-mRNA spliceosome (PDB:6QX9), cross-link satisfaction was determined to be 91% (40/44) and 86% (37/43), respectively (Figure 5B–D). Collectively, these results suggest that most DBrASO cross-links matched well with known protein structures, in line with results obtained using lysine-reactive cross-linkers.[10,13–15]

DBrASO XL-PPI Network of HEK 293 Cell Lysates

To visualize the identified PPIs, we generated an XL-PPI network comprising 505 nodes and 856 edges, denoting 856 interprotein interactions (Figure S7A). Although the number of XL-PPIs captured by DBrASO and DSSO is similar (856 vs. 855), their overlap is only 4.5% (Figure S7B), suggesting substantial differences in PPI mapping. For the 323 XL-PPIs that are present in the STRING database, more than 86% have a STRING score above 0.9 (Figure S8), which is similar to other proteome-wide XL-MS results,[14,15] suggesting high confidence in the PPIs captured by DBrASO cross-linking. In comparison to current BioPlex and BioGrid databases as well as the published proteome-wide XL-MS data,[10,13–15] 570 out of the identified 856 PPIs are known and 286 are novel (Table S4).

Among the novel PPIs, 128 correspond to interactions involving ribosomal proteins. For instance, multiple interaction contacts between UBA52 and 40S/60S ribosomal proteins were uniquely identified by DBrASO cross-linking but not by lysine-reactive reagents. This is due to the fact that the N-terminus of UBA52 (also called ubiquitin-60S ribosomal protein L40) has identical sequence to ubiquitin (1–76 AA). Thus, any cross-linked peptides involving the N-terminus of UBA52 (1–76) would be ambiguous as they could belong to ubiquitin and/or other ubiquitin precursors. While multiple lysines exist at the C-terminus (77–128 AA) of UBA 52, cross-linked peptides involving the C-terminus have not been reported using lysine-reactive cross-linkers. Here, cysteine XL by DBrASO produced physical evidence to support the direct interaction of UBA52 with ribosomal proteins due to the identification of its unique C-terminal peptide (^{115}CGHTNNLRPK^{124}).

Additionally, 34 novel interactions identified here are related to GAPDH, including its interactions with heat shock proteins, 40S ribosomal, 60S ribosomal, TRiC-complex, and other proteins (Figure 6). All these interactions involve C247 of GAPDH, indicating that

this region is in proximity to GAPDH interactors. Although GAPDH is a relatively abundant protein, its interactions with other proteins have rarely been described in previous DSSO XL-MS datasets of cell lysates.[10,13,15] While enrichable lysine-reactive Alkyne-A-DSBSO was able to capture several GAPDH related PPIs,[14] only 2 PPIs were shared with those captured by DBrASO (GAPDH-HNRNPDL and GAPDH-RPL30). Interestingly, 29 out of the 65 interprotein DSBSO K-K linkages from GAPDH involve K251, K259, K260 and K263,[14] which are very close to C247 in both sequence and structure, reaffirming GADPH interactions captured by DBrASO in HEK293 cell lysates.

Moreover, an interaction between CCT2:C535 and TUBB:C12 was identified, which was not uncovered by previous lysine-reactive XL-MS studies.[10,13–15] While it is known that CCT complex regulates the folding of tubulin,[40] the details in their physical interactions have not been reported before. The proximity between the C-terminus of CCT2 to N-terminus of TUBB identified here correlates well with a recently published 3-D structure of nanobody and tubulin bound human TRiC complex (PDB: 7NVN) although the complete C-terminal structure of CCT2 was not fully resolved. Collectively, our results have demonstrated the complementarity of DBrASO cross-linking to lysine-reactive reagents in proteome-wide PPI profiling.

CONCLUSION

In this study, we have designed and synthesized a novel sulfoxide-containing MS-cleavable cysteine reactive cross-linker, DBrASO, which has been extensively characterized by a synthetic peptide and standard protein BSA. The results have demonstrated that DBrASO cross-linked peptides carry the same MS-cleavable characteristics as other sulfoxide-containing MS-cleavable cross-linkers and can be identified unambiguously using LC-MS^n workflow.[5,14,18,19,29,32] In comparison to our previously developed maleimide-based MS-cleavable cross-linker BMSO,[19] DBrASO possesses better specificity at physiological pH, which is beneficial for complex PPI mapping at the proteome level. In addition, bromoacetamide is non-hydrolyzable and produces more homogenous cross-linked products that would be beneficial for future quantitative XL-MS studies. Importantly, we have successfully demonstrated the feasibility of DBrASO in proteome-wide PPI profiling of cell lysates and its potential in complementing existing reagents especially lysine-reactive cross-linkers. To the best of our knowledge, this work represents the first proteome-wide PPI studies using non-lysine-reactive cross-linkers and has established a solid foundation for us to further expand the coverage of XL-proteomes at the systems-level.

Supplementary Material

Refer to Web version on PubMed Central for supplementary material.

Acknowledgments

We wish to thank Prof. A.L. Burlingame, Drs. Peter Baker and Robert Chalkley for their support of Protein Prospector. This work was supported by National Institutes of Health grants R35GM145249, R01GM074830 and R01GM130144 to L.H. and a National Science Foundation Grant CHE-1807612 to S.D.R..

Data Availability

Data are available at the PRIDE database with identifier PXD037443

Username: reviewer_pxd037443@ebi.ac.uk

Password: MUHq9Ikp

ABBREVIATIONS

XL-MS	cross-linking mass spectrometry
BMSO	**bi**s**m**aleimide **s**ulf**o**xide, a.k.a. 3,3’-sulfinylbis(N-(2-(2,5-dioxo-2,5-dihydro-1H-pyrrol-1-yl)ethyl)propanamide
DSSO	**d**i**s**uccinimidyl **s**ulf**o**xide
DHSO	**d**i**h**ydrazide **s**ulf**o**xide a.k.a., 3,3’-sulfinyldi(propanehydrazide)
Azide/Alkyne-A-DSBSO	**B**SO/Alkene-tagged, **a**cid-cleavable **d**i**s**uccinimidyl **b**is-**s**ulf**o**xide
DBrASO	**d**i**br**omo**a**cetamide **s**ulf**o**xide (3,3’-sulfinylbis(*N*’-(2-bromoacetyl)-propanehydrazide)
MS	mass spectrometry
MS^n	multi-stage mass spectrometry
CID	collisional induced dissociation
LC-MS^n	liquid chromatography multistage mass spectrometry
CSM	cross-link peptide spectrum match
PPI	protein-protein interaction
SEC-HpHt	size-exclusion chromatography coupled with high pH reverse phase tip fractionation

REFERENCES

(1). Alberts B The cell as a collection of protein machines: preparing the next generation of molecular biologists. cell 1998, 92, 291–294. [PubMed: 9476889]

(2). Leitner A; Faini M; Stengel F; Aebersold R Crosslinking and mass spectrometry: an integrated technology to understand the structure and function of molecular machines. Trends in biochemical sciences 2016, 41, 20–32. [PubMed: 26654279]

(3). Liu F; Rijkers DT; Post H; Heck AJ Proteome-wide profiling of protein assemblies by cross-linking mass spectrometry. Nature methods 2015, 12, 1179–1184. [PubMed: 26414014]

(4). Iacobucci C; Götze M; Ihling CH; Piotrowski C; Arlt C; Schaefer M; Hage C; Schmidt R; Sinz A A cross-linking/mass spectrometry workflow based on MS-cleavable cross-linkers and the MeroX software for studying protein structures and protein-protein interactions. Nature protocols 2018, 13, 2864–2889. [PubMed: 30382245]

(5). Yu C; Huang L Cross-linking mass spectrometry (XL-MS): An emerging technology for interactomics and structural biology. Analytical chemistry 2018, 90, 144. [PubMed: 29160693]

(6). Chavez JD; Wippel HH; Tang X; Keller A; Bruce JE In-Cell Labeling and Mass Spectrometry for Systems-Level Structural Biology. Chem Rev 2021, 122, 7647–7689.. [PubMed: 34232610]

(7). Herzog F; Kahraman A; Boehringer D; Mak R; Bracher A; Walzthoeni T; Leitner A; Beck M; Hartl F-U; Ban N Structural probing of a protein phosphatase 2A network by chemical cross-linking and mass spectrometry. Science 2012, 337, 1348–1352. [PubMed: 22984071]

(8). Gutierrez C; Chemmama IE; Mao H; Yu C; Echeverria I; Block SA; Rychnovsky SD; Zheng N; Sali A; Huang L Structural dynamics of the human COP9 signalosome revealed by cross-linking mass spectrometry and integrative modeling. Proceedings of the National Academy of Sciences 2020, 117, 4088–4098.

(9). Hage C; Iacobucci C; Rehkamp A; Arlt C; Sinz A The first zero-length mass spectrometry-cleavable cross-linker for protein structure analysis. Angewandte Chemie 2017, 129, 14743–14747.

(10). Liu F; Lössl P; Scheltema R; Viner R; Heck AJ Optimized fragmentation schemes and data analysis strategies for proteome-wide cross-link identification. Nature communications 2017, 8, 1–8.

(11). Chavez JD; Lee CF; Caudal A; Keller A; Tian R; Bruce JE Chemical crosslinking mass spectrometry analysis of protein conformations and supercomplexes in heart tissue. Cell systems 2018, 6, 136–141. [PubMed: 29199018]

(12). Steigenberger B; van den Toorn HW; Bijl E; Greisch J-F; Räther O; Lubeck M; Pieters RJ; Heck AJ; Scheltema RA Benefits of collisional cross section assisted precursor selection (caps-PASEF) for cross-linking mass spectrometry. Molecular & Cellular Proteomics 2020, 19, 1677–1687. [PubMed: 32694122]

(13). Yugandhar K; Wang T-Y; Leung AK-Y; Lanz MC; Motorykin I; Liang J; Shayhidin EE; Smolka MB; Zhang S; Yu H MaXLinker: proteome-wide cross-link identifications with high specificity and sensitivity. Molecular & Cellular Proteomics 2020, 19, 554–568. [PubMed: 31839598]

(14). Wheat A; Yu C; Wang X; Burke AM; Chemmama IE; Kaake RM; Baker P; Rychnovsky SD; Yang J; Huang L Protein interaction landscapes revealed by advanced in vivo cross-linking-mass spectrometry. Proceedings of the National Academy of Sciences 2021, 118.

(15). Jiao F; Yu C; Wheat A; Wang X; Rychnovsky SD; Huang L Two-Dimensional Fractionation Method for Proteome-Wide Cross-Linking Mass Spectrometry Analysis. Analytical chemistry 2022, 94, 4236–4242. [PubMed: 35235311]

(16). Ihling CH; Piersimoni L; Kipping M; Sinz A Cross-linking/mass spectrometry combined with ion mobility on a timsTOF Pro instrument for structural proteomics. Analytical Chemistry 2021, 93, 11442–11450. [PubMed: 34375526]

(17). Sarnowski CP; Bikaki M; Leitner A Cross-linking and mass spectrometry as a tool for studying the structural biology of ribonucleoproteins. Structure 2022.

(18). Gutierrez CB; Yu C; Novitsky EJ; Huszagh AS; Rychnovsky SD; Huang L Developing an acidic residue reactive and sulfoxide-containing MS-cleavable homobifunctional cross-linker for probing protein-protein interactions. Analytical chemistry 2016, 88, 8315–8322. [PubMed: 27417384]

(19). Gutierrez CB; Block SA; Yu C; Soohoo SM; Huszagh AS; Rychnovsky SD; Huang L Development of a novel sulfoxide-containing MS-cleavable homobifunctional cysteine-reactive cross-linker for studying protein-protein interactions. Analytical chemistry 2018, 90, 7600–7607. [PubMed: 29792801]

(20). Barford D The role of cysteine residues as redox-sensitive regulatory switches. Current opinion in structural biology 2004, 14, 679–686. [PubMed: 15582391]

(21). Marino SM; Gladyshev VN Analysis and functional prediction of reactive cysteine residues. Journal of Biological Chemistry 2012, 287, 4419–4425. [PubMed: 22157013]

(22). Poole LB The basics of thiols and cysteines in redox biology and chemistry. Free Radical Biology and Medicine 2015, 80, 148–157. [PubMed: 25433365]

(23). Bak DW; Bechtel TJ; Falco JA; Weerapana E Cysteine reactivity across the subcellular universe. Current opinion in chemical biology 2019, 48, 96–105. [PubMed: 30508703]

(24). Sornay C; Vaur V; Wagner A; Chaubet G An overview of chemo-and site-selectivity aspects in the chemical conjugation of proteins. Royal Society Open Science 2022, 9, 211563. [PubMed: 35116160]

(25). Baldwin AD; Kiick KL Tunable degradation of maleimide-thiol adducts in reducing environments. Bioconjugate chemistry 2011, 22, 1946–1953. [PubMed: 21863904]

(26). Brewer CF; Riehm JP Evidence for Possible Nonspecific Reactions between N-Ethylmaleimide and Proteins. Analytical Biochemistry 1967, 18, 248–255.

(27). Shevchenko A; Wilm M; Vorm O; Mann M Mass spectrometric sequencing of proteins from silver-stained polyacrylamide gels. Analytical chemistry 1996, 68, 850–858. [PubMed: 8779443]

(28). Weerapana E; Wang C; Simon GM; Richter F; Khare S; Dillon MB; Bachovchin DA; Mowen K; Baker D; Cravatt BF Quantitative reactivity profiling predicts functional cysteines in proteomes. Nature 2010, 468, 790–795. [PubMed: 21085121]

(29). Kao A; Chiu C.-l.; Vellucci D; Yang Y; Patel VR; Guan S; Randall A; Baldi P; Rychnovsky SD; Huang L Development of a Novel Cross-linking Strategy for Fast and Accurate Identification of Cross-linked Peptides of Protein Complexes. Molecular & Cellular Proteomics 2011, 10.

(30). Müller T; Winter D Systematic evaluation of protein reduction and alkylation reveals massive unspecific side effects by iodine-containing reagents. Molecular & cellular proteomics 2017, 16, 1173–1187. [PubMed: 28539326]

(31). Murphy EL; Joy AP; Ouellette RJ; Barnett DA Optimization of cysteine residue alkylation using an on-line LC-MS strategy: Benefits of using a cocktail of haloacetamide reagents. Analytical Biochemistry 2021, 619, 114137. [PubMed: 33582115]

(32). Kaake RM; Wang X; Burke A; Yu C; Kandur W; Yang Y; Novtisky EJ; Second T; Duan J; Kao A A new in vivo cross-linking mass spectrometry platform to define protein–protein interactions in living cells. Molecular & Cellular Proteomics 2014, 13, 3533–3543. [PubMed: 25253489]

(33). Yu C; Kandur W; Kao A; Rychnovsky S; Huang L Developing new isotope-coded mass spectrometry-cleavable cross-linkers for elucidating protein structures. Analytical chemistry 2014, 86, 2099–2106. [PubMed: 24471733]

(34). Götze M; Iacobucci C; Ihling CH; Sinz A A simple cross-linking/mass spectrometry workflow for studying system-wide protein interactions. Analytical chemistry 2019, 91, 10236–10244. [PubMed: 31283178]

(35). Lenz S; Sinn LR; O'Reilly FJ; Fischer L; Wegner F; Rappsilber J Reliable identification of protein-protein interactions by crosslinking mass spectrometry. Nature communications 2021, 12, 1–11.

(36). Shi Y; Fernandez-Martinez J; Tjioe E; Pellarin R; Kim SJ; Williams R; Schneidman-Duhovny D; Sali A; Rout MP; Chait BT Structural characterization by cross-linking reveals the detailed architecture of a coatomer-related heptameric module from the nuclear pore complex. Molecular & Cellular Proteomics 2014, 13, 2927–2943. [PubMed: 25161197]

(37). Gutierrez C; Salituro LJ; Yu C; Wang X; DePeter SF; Rychnovsky SD; Huang L Enabling Photoactivated Cross-linking Mass Spectrometric Analysis of Protein Complexes by Novel MS-cleavable Cross-linkers. Molecular & Cellular Proteomics 2021, 20.

(38). Wilhelm M; Schlegl J; Hahne H; Gholami AM; Lieberenz M; Savitski MM; Ziegler E; Butzmann L; Gessulat S; Marx H Mass-spectrometry-based draft of the human proteome. Nature 2014, 509, 582–587. [PubMed: 24870543]

(39). Tüting C; Iacobucci C; Ihling CH; Kastritis PL; Sinz A Structural analysis of 70S ribosomes by cross-linking/mass spectrometry reveals conformational plasticity. Scientific reports 2020, 10, 1–13. [PubMed: 31913322]

(40). Muñoz IG; Yébenes H; Zhou M; Mesa P; Serna M; Park AY; Bragado-Nilsson E; Beloso A; De Cárcer G; Malumbres M Crystal structure of the open conformation of the mammalian chaperonin CCT in complex with tubulin. Nature structural & molecular biology 2011, 18, 14–19.

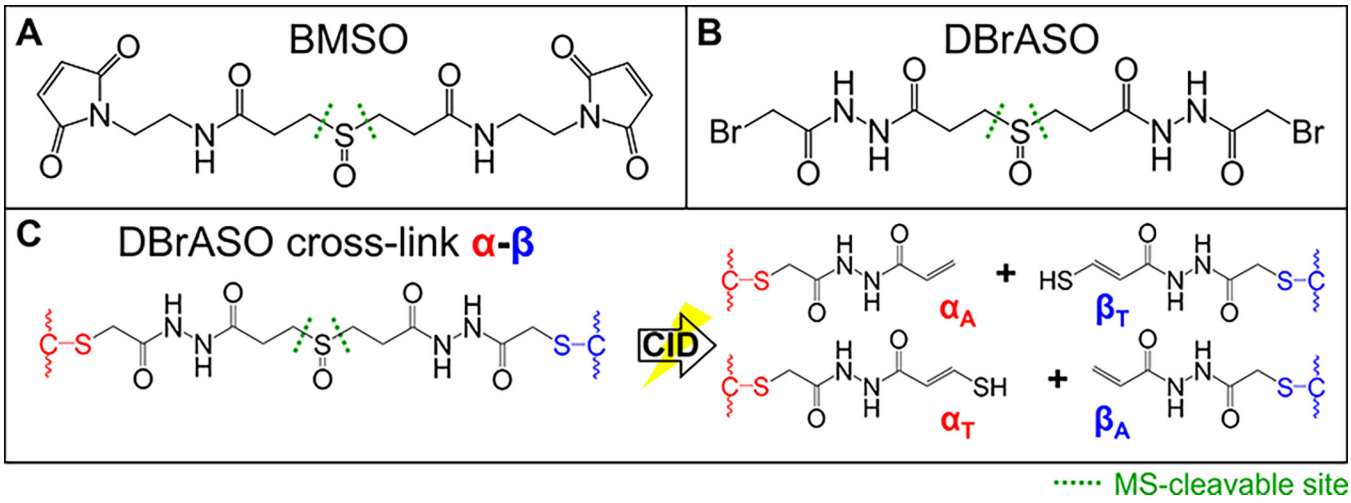

Figure 1.

Schematics of the sulfoxide-containing MS-cleavable cysteine reactive cross-linkers. Structures of (A) BMSO and (B) DBrASO. (C) Predicted MS^2 fragmentation of a DBrASO interlinked peptide.

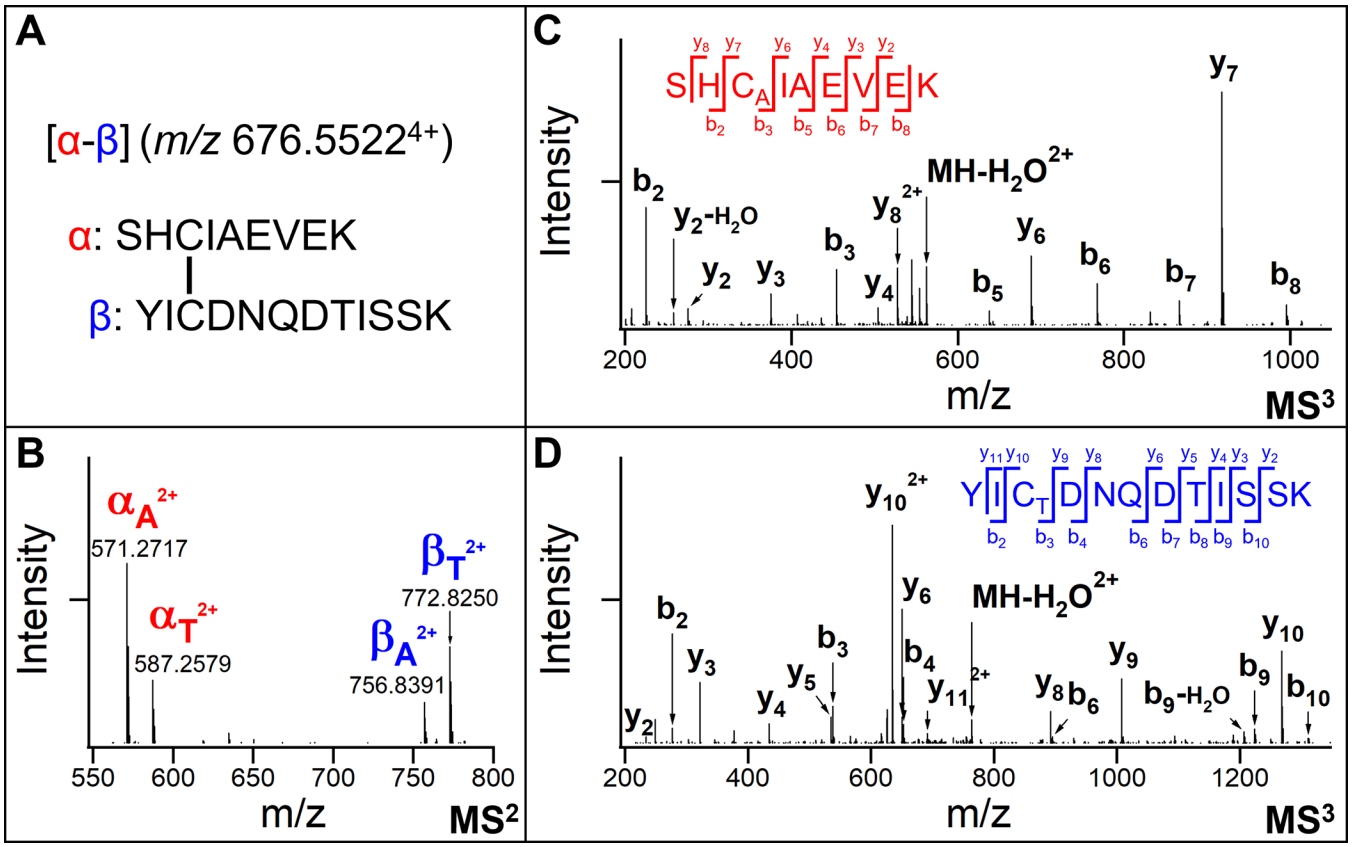

Figure 2.

MS^n analysis of a representative DBrASO interlinked peptide of BSA. (A) DBrASO interlinked peptide was detected as a quadruply charged ion (α-β) (m/z 676.5522^{4+}) in MS^1. (B) MS^2 spectrum of the cross-linked peptide (α-β) in (A), in which two expected fragment ion pairs were detected, α_A/β_T (m/z 571.2717^{2+}/772.8250^{2+}) and α_T/β_A (m/z 587.2579^{2+}/756.8391^{2+}). (C) MS^3 analysis of α_A (m/z 571.2717^{2+}) identified the sequence as SHC$_A$IAEVEK, in which the cysteine residue was modified with alkene (A). (D) MS^3 analysis of β_T (m/z 772.8250^{2+}) identified the sequence as YIC$_T$DNQDTISSK, in which the cysteine residue was modified with thiol (T).

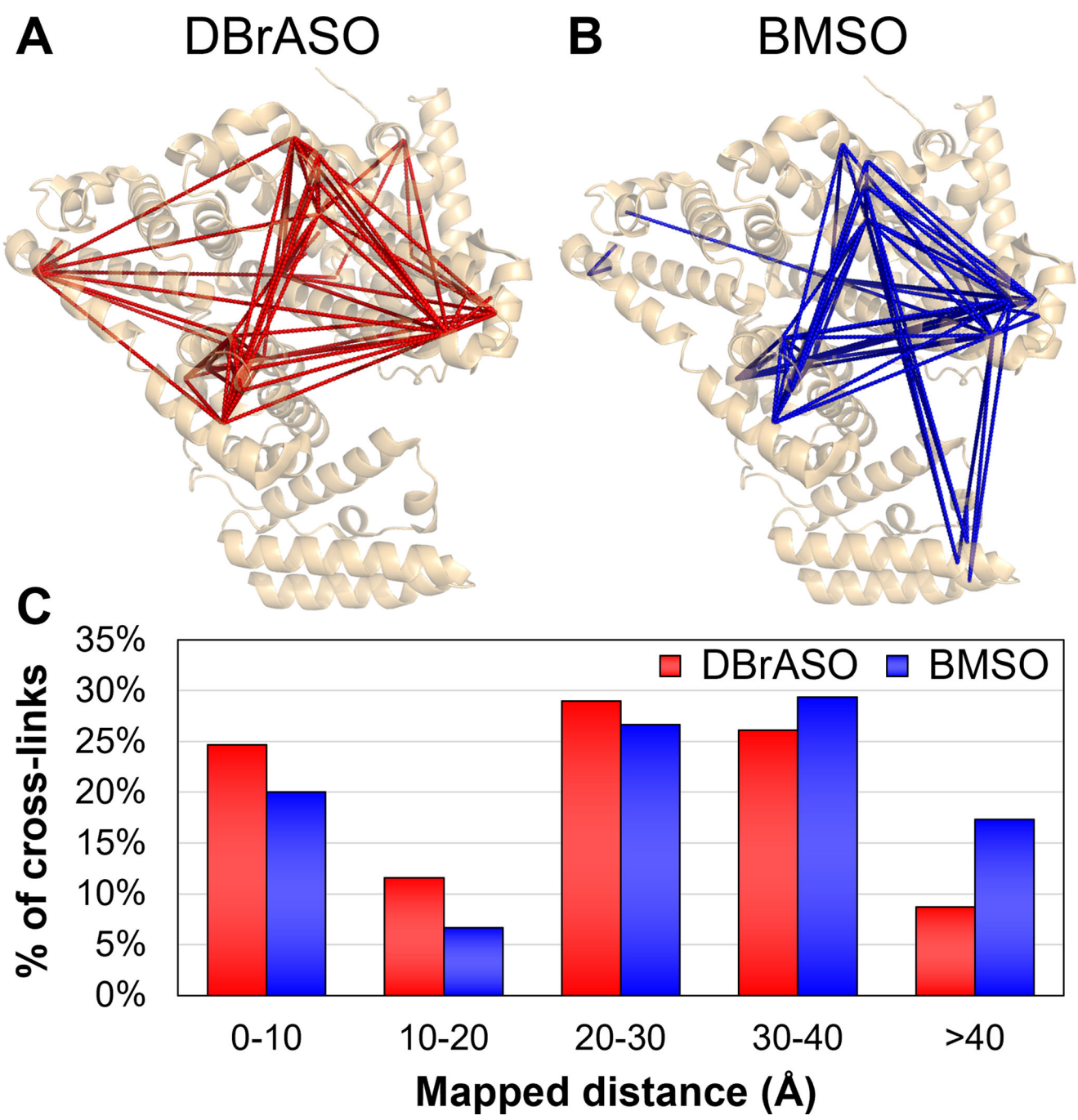

Figure 3.

C-C XL-maps of BSA (PDB: 4F5S). Three-dimensional (3-D) XL-map from (A) DBrASO (Red) and (B) BMSO (Blue) cross-linked data. (C) Distance distribution plots of DBrASO (red) and BMSO (blue) C-C linkages.

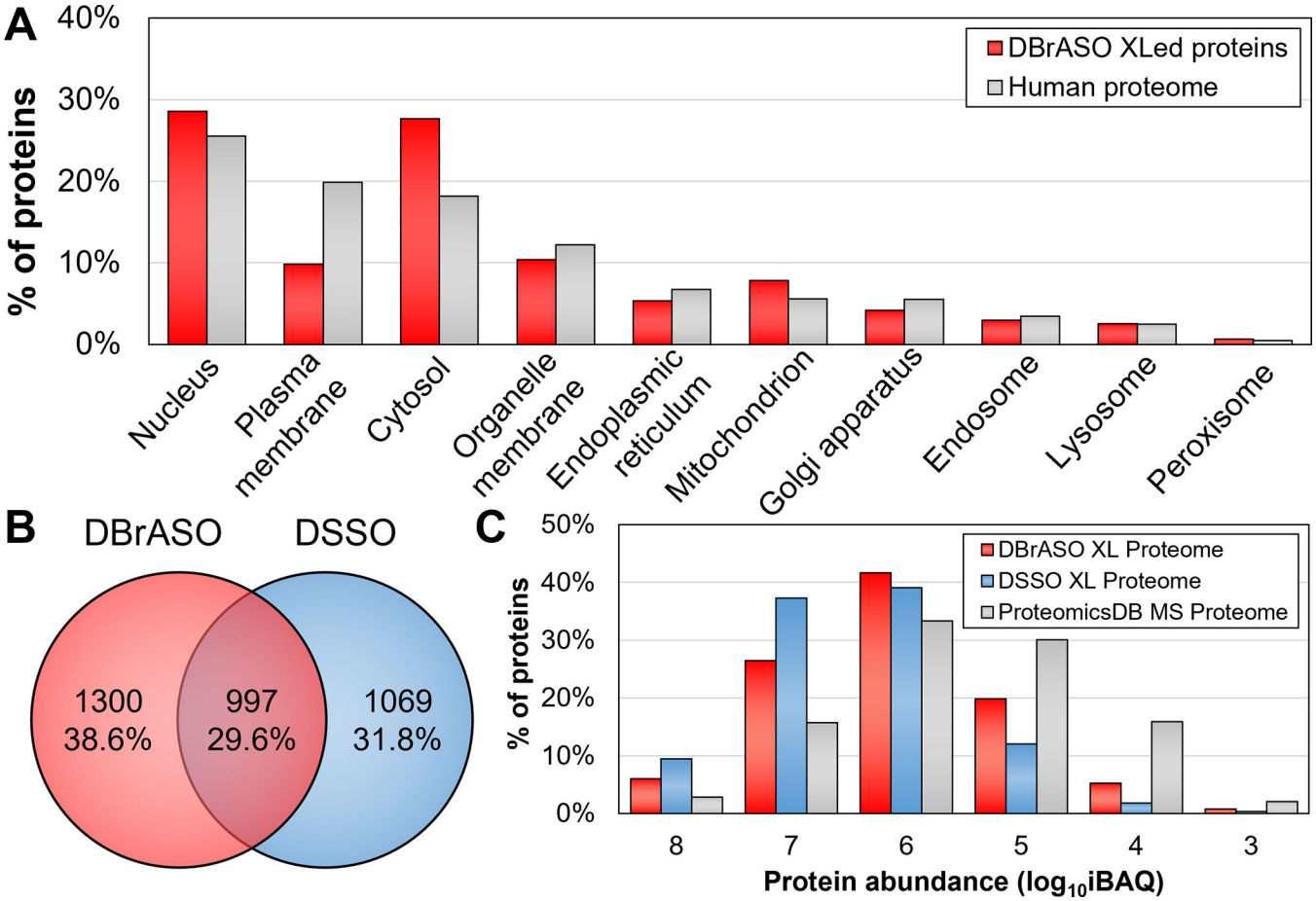

Figure 4.

Comparison of DBrASO and DSSO XL-Proteomes of HEK 293 cell lysates. (A) Subcellular compartment distribution of Human proteome (from uniprot) and DBrASO cross-linked proteins. (B) Overlap of DSSO and DBrASO cross-linked proteins. (C) iBAQ-based abundance distribution of DBrASO (red) and DSSO (blue) XL-proteomes, and MS-proteome from Proteomics DB (grey).

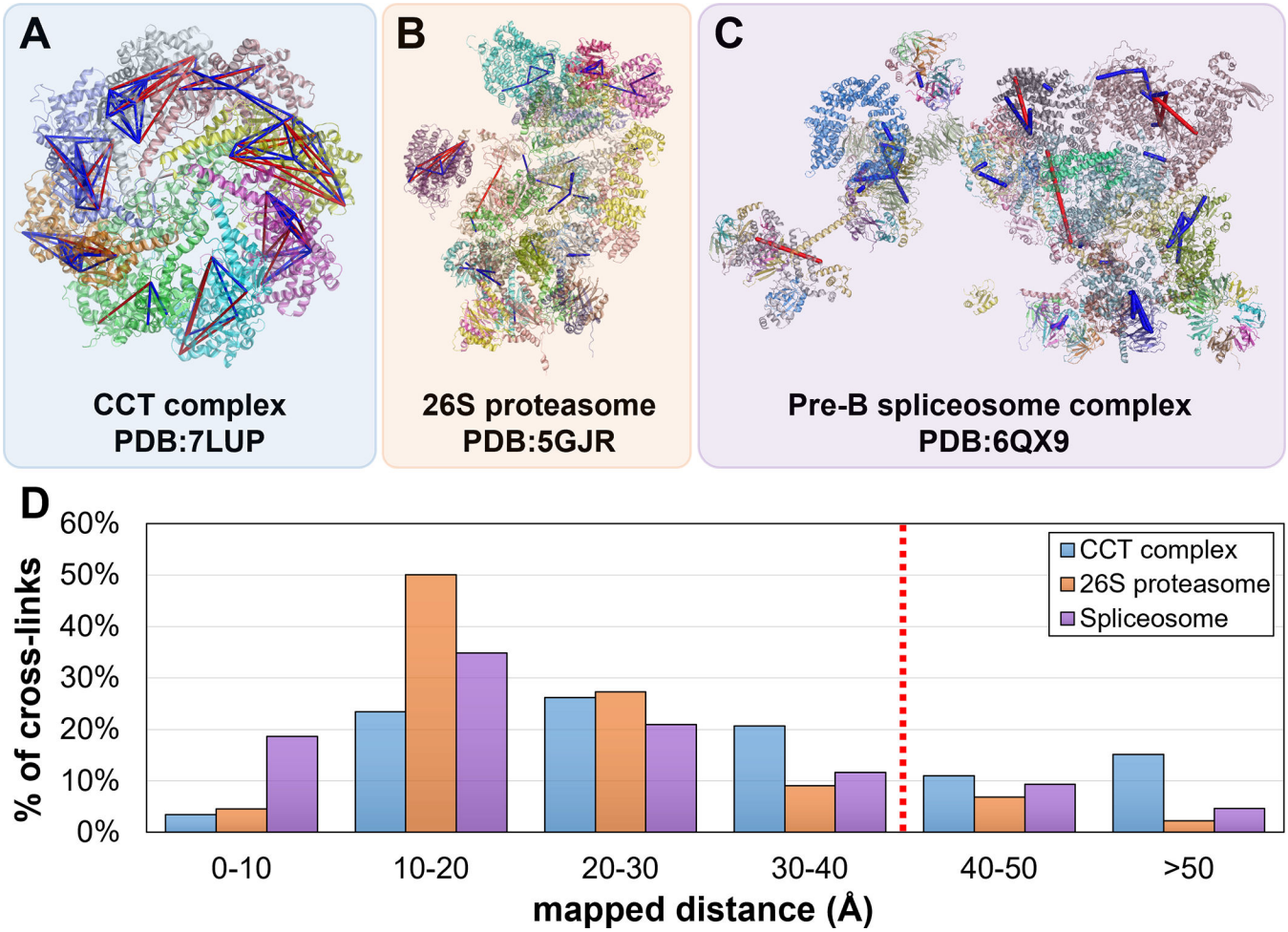

Figure 5.

Evaluation of C-C cross-links by structural mapping. Mapping DBrASO cross-links onto high-resolution 3D structures of (A) the CCT complex (PDB: 7LUP), (B) 26S proteasome (PDB: 5GJR), and (C) pre-B spliceosome complex (PDB: 6QX9). Satisfied cross-links (≤ 40 Å) were labeled blue and non-satisfied cross-linked (> 40 Å) were labeled red. (D) Distance distributions of the identified cross-links from the three selected complexes.

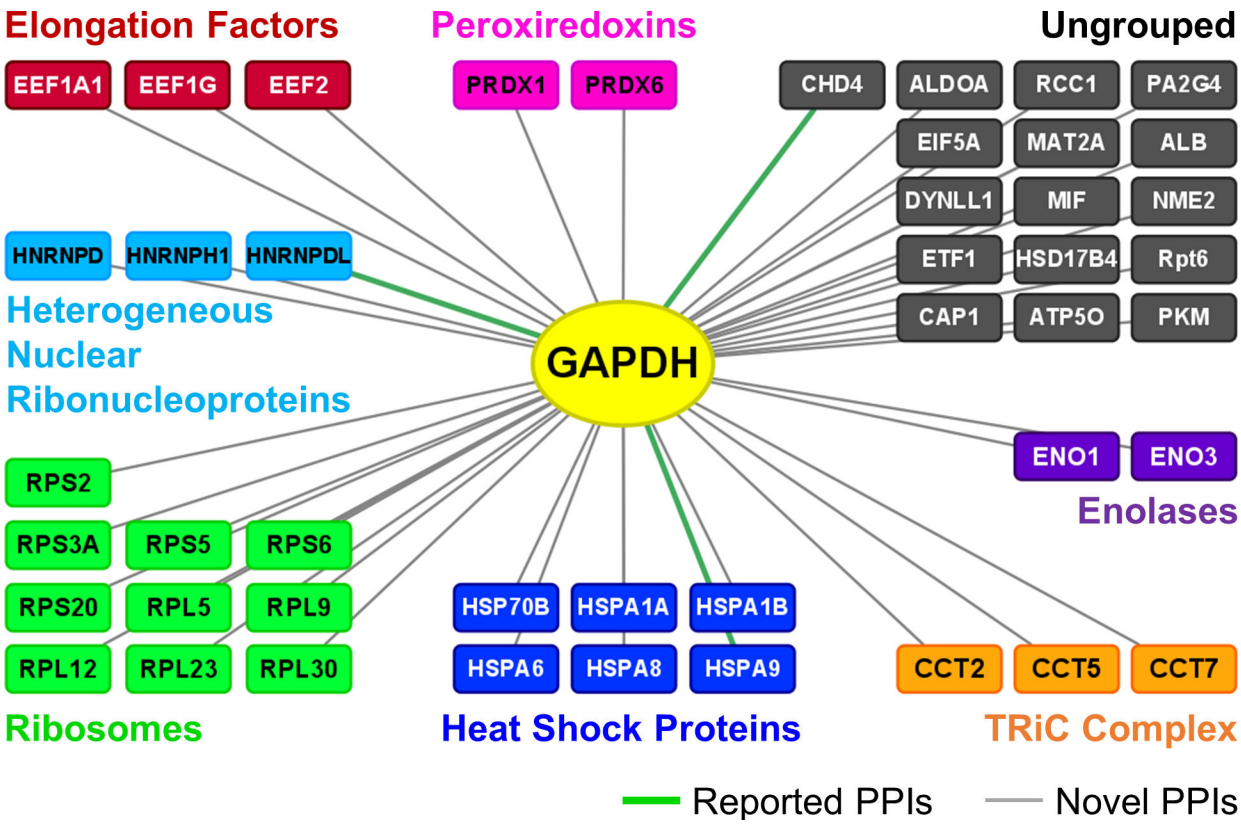

Figure 6.

GAPDH-containing XL-PPI networks by DBrASO cross-linking. GAPDH-interacting proteins were grouped by protein families. The reported PPIs were labeled by grey edges, and the novel PPIs were labeled by green edges.